 doi:10.20944/preprints201911.0125.v1

Article

Estimating Zonal Ekman Transport along Coastal Senegal during Passage of Hurricane Fred (2015) from August 30 to 31, 2015

Abdou Lahat Dieng [1], Siny Ndoye [1], Gregory S. Jenkins [2]. Saïdou M. Sall [1] and Amadou T. Gaye [1]

[1] Laboratoire de Physique de l'Atmosphère et de l'Océan Siméon-Fongang, Ecole Supérieure Polytechnique, Université Cheikh Anta Diop
[2] Department of Meteorology, The Pennsylvania State University, University Park, Pennsylvania.
Correspondence: abdoulahat.dieng@ucad.edu.sn

Abstract: We examine the role of zonal Ekman transport along the coast of Senegal on 30 August, 2015 when the tropical disturbance associated with Tropical Cyclone Fred was located to the west of Senegal causing considerable coastal damage to coastal areas south of Dakar, Senegal. Ten-meter winds from three Weather Research and Forecast model simulations were used to estimate zonal Ekman transport, with the largest values found during the 30 August. The simulations are in agreement with limited coastal observations showing increasing southerly wind speeds during 30 August but are overestimated relative to the 3 coastal stations. The strong meridional winds translate into increased zonal Ekman transport to the coast of Senegal on 30 August. The use of a coupled ocean model will improve the estimates of Ekman transport along the Guinea-Senegalese coast. The observed damage suggests that artificial and natural barriers (mangroves) should be strengthened to protect coastal communities in Senegal.

Keywords: tropical cyclone; Weather Research and Forecast model; zonal Ekman transport

 doi:10.20944/preprints201911.0125.v1

1. Introduction

Coastal Resilience in West Africa and the nearby Islands of Cabo Verde are challenging because of mounting human drivers associated with population growth, socio-economic development, natural hazards, anthropogenic climate change, and limited observing systems. An estimated 100 million persons live along coastal West Africa, which is expected to increase throughout the 21st century rapidly. Most of the region has a limited observing network along coastlines and also over the oceans. Ship reports provide most of the real-time ocean and weather conditions between Cape Verde and Coastal West Africa; while the Prediction and Research Moored Array in the Tropical Atlantic (PIRATA) of buoys are sufficiently far from coastal zones in West Africa[1]. There are limited tide-gauges and coastal weather stations along coastal West Africa. Automated weather stations in Cape Verde were critical to observing Hurricane Fred Observations of coastal flooding from sea-level rise and natural hazards [2].

During the northern hemisphere summer season, African Easterly Waves (AEWs) move across West Africa every 3-5 days and may be associated with flooding inland but can evolve further to tropical disturbances over the Atlantic Ocean [3,4]. Sometimes, an area of low pressure, with a well-defined area of vorticity between 850-700 hPa can develop after the AEWs exits the coast leading to a tropical depression or a named storm. In 1999, the disturbance associated with Tropical cyclone Cindy was observed from Senegal and lead to more than 100 fatalities along the coast of Senegal and Mauritania [5]. Senegal is located in the Western Sahel, with a growing population of approximately 15 million residents. However, many of the residents live near the capital of Dakar, which is the westernmost city along the African Coast (14.59N, 17.5W). More than 20% of the Senegalese population lives in Dakar although it does not cover more than 0.5% of country's are, according to the latest report from the National Agency for Statistics and Demography of Senegal (http://www.ansd.sn/). Senegal has a coastline of 706.72 km long [6] and the waters are enriched along the continental shelf by upwelling (which starts in October and ends in late May to early June), which ensures high primary production [7–10]. Therefore, artisanal fishing is the first economic activity generating income in Senegal.

Two types of swells characterize the Senegalese coast: (1) In the northern zone (between St-Louis and Dakar) the trade winds and disturbances of the North Atlantic basin generate swells of north/northwest direction throughout the year. (2) In the southern zone (from Dakar to Cap-Skirring), swells are less frequent because northwest Atlantic swells are diffracted over the peninsula of Cape Verde (defined has the Region of Dakar) which considerably weakens them. However, swells occur mostly in NH summer period and can be generated by Mesoscale convective systems and/or African Easterly Waves which can deepen into tropical depressions off the coast [2,5,11,12]. The consequences can be disastrous for the populations living along the littoral. Indeed, this zone is characterized by a broad and shallow continental shelf (i.e., 20–30 m over tens of kilometers, figure 2b) compared to the northern zone [8,13]. The shallow depth of the ocean and the concave shape of Senegal's coastline can lead to the gradual advance of the sea, thereby increasing coastal population vulnerability to flooding during strong swell events.

Hurricanes rarely occur in the extreme Eastern Atlantic Ocean but on 31 August 2015, Hurricane Fred passed through the Cape Verde Islands, causing damage in seven of the ten Islands [2]. This storm rapidly intensified from a tropical depression at 0000 UTC on 30 August to a hurricane 0000 UTC 31 August. However, prior to reaching Cape Verde, this storm caused seven fatalities

 doi:10.20944/preprints201911.0125.v1

associated with a fishing vessel and caused damage along with Senegalese coastline. During 30 August, 2015 reports by administrative authorities of Fatick region, which is in southwest Senegal reported significant losses in the villages (Palmarin, Sessene, Dionewar, Ngallou, Diakhanor, Djifere, Cap Skirring) caused by a strong swell during the night of 30 August (figure 2b). They report that approximately 20 houses were destroyed displacing many people. Further north, media reports suggest that more than 200 home were damaged/destroyed along with boats. Residents that were interviewed in Bargny, Senegal and the Hann District of Senegal spoke of the rise of the seas during the day of 30 August leading to widespread destruction (figure 1b,1c and 1d).

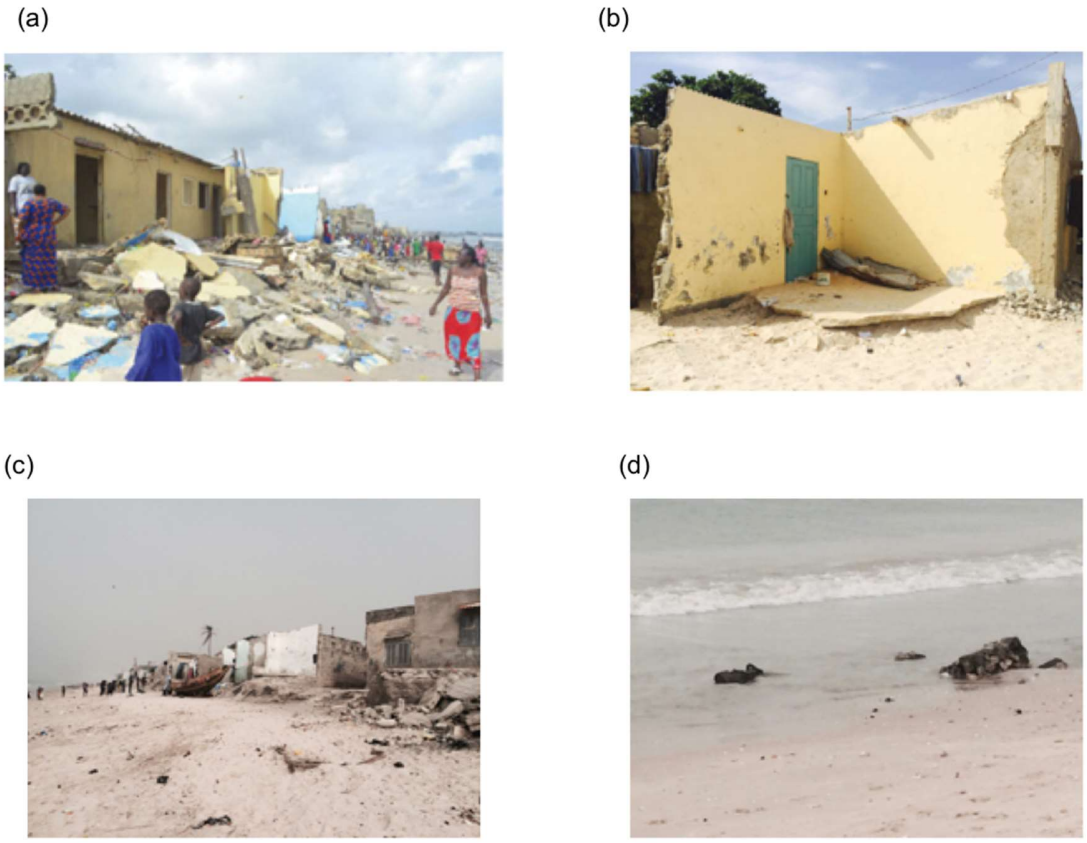

Figure 1: Illustrations of the damage caused by the passage of Hurricane Fred in the night of 30 August 2015 off the coast of Senegal: (a) in Thiaroye; (b), (c), and (d) in Bargny.

The black dashed line in figure 2a shows the evolution and track of tropical disturbance associated with Fred making the closest approach to West Africa near the Guinea-Bissau at 0000 UTC 30 August. Throughout the day, TC Fred is located several hundred kilometers off the coast of Senegal, and by 0000 31 August, the center of then Hurricane Fred is located approximately at 4.2 degrees west of Dakar according to NHC archives.

Preprints (www.preprints.org) | NOT PEER-REVIEWED | Posted: 12 November 2019 doi:10.20944/preprints201911.0125.v1

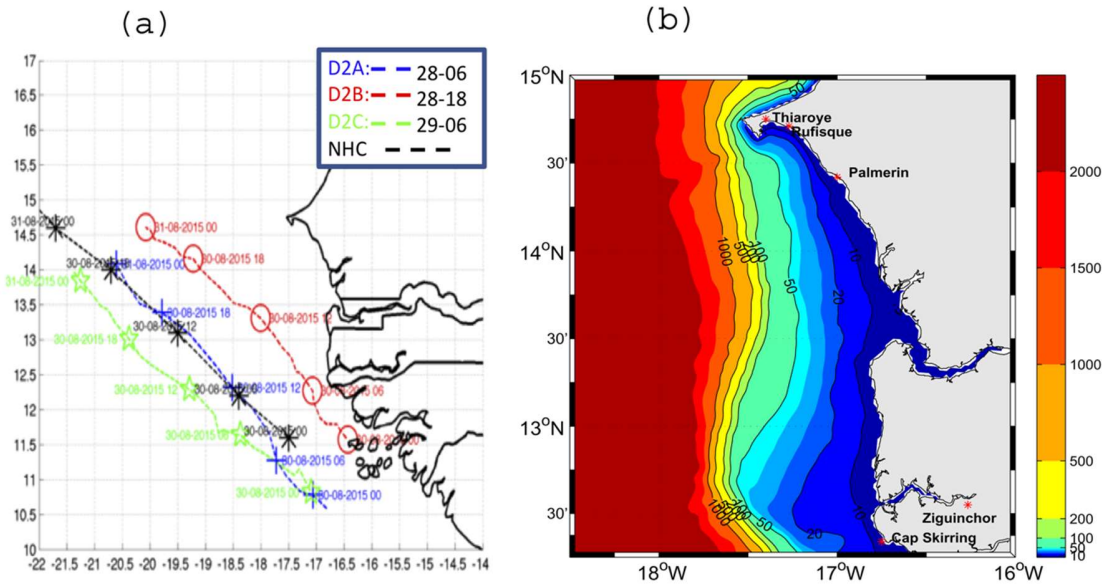

Figure 2: (a) Evolution and track of tropical disturbance associated with Fred from August 30, 2015 at 0000 UTC to August 31, 2015 at 0000 UTC ; (b) the ocean bathymetry (m) off southern Senegal and Gambia coast is represented in color. Isobaths are indicated from 10 to 1000 m depth (Black lines labelled with depth in meters

The objectives of this work are to use a set of fine grid spacing simulations using the Weather, Research and Forecasting (WRF) model to characterize the disturbance associated with TC Fred through the period of 29 and 30 August during its evolution. We then use WRF output from these simulations to estimate Ekman transport of water towards the coast of Senegal that could have been associated with coastal damage on 30 August 2015. This paper is organized as follows: the used data, model simulations and Ekman transport estimates are presented in Section 2. The results and conclusions are presented in Sections 3 and 4.

2. Data, model Simulations and Ekman Transport estimates.

The new gridded daily-averaged wind and wind stress fields (DASCAT), estimated over global oceans from ASCAT retrievals using objective method is used to examine 10 m wind associated to Fred genesis. Data have spatial resolutions of 0.25° in longitude and latitude. The calculation of daily estimates uses ascending as well as descending available and valid retrievals. According to the ASCAT sampling scheme, the objective method allowing the determination of regular in space and surface wind fields uses ASCAT observations as well as ECMWF analyses. The latter are considered as the temporal interpolation basis of ASCAT retrievals. More details about data, objective method, computation algorithm may be found in [14]. Satellite infrared Brightness Temperature from Meteosat Second Generation, ERA-Interim reanalyzed fields [15] and Reynold Sea Surface Temperature [16]are used to analyze environmental conditions leading to the genesis of hurricane Fred.

The wind measured at Dakar airport representative of the winds over the Southern Senegal [8,17] are also used to evaluate the ability of the Weather Research and Forecasting (WRF) model to reproduce the surface wind circulations over the southern Senegalese coast.

Preprints (www.preprints.org) | NOT PEER-REVIEWED | Posted: 12 November 2019 doi:10.20944/preprints201911.0125.v1

To examine the role of Ekman Transport, we use the Weather Research and Forecasting (WRF) model, which has an outer 12 km grid spacing domain and an inner 4 km grid spacing domain. We use the WRF version 3.71 [18] in this study to examine the tropical disturbance off the coast of West Africa. The National Center for Environmental Prediction (NCEP) final analyses FNL is used initialize and provide boundary conditions using FNL analyses for the parent domain at 12 km every 6 hours. Three simulations using two domains are used in simulating TC Fred. The simulations are started at different times beginning on 28 August 0000 UTC and initialized every 12 hours (Table 1). The coarse grid has 12 km grid spacing with 31 vertical levels, 251 east-west grid points, and 181 north-south grid points covering much of West Africa and the extreme Eastern Atlantic. The fine grid uses 4 km grid spacing with 31 vertical levels, 196 east-west points and 160 north-south points covering Senegal and extreme Eastern Atlantic (Table 1). The fine grid simulations begin 6 hours after the course grid simulation is initiated. There is two-way feedback used between the coarse and fine grid domains. The larger domain uses the Kain-Fritsch cumulus parameterization, while the inner domain does not use a cumulus parameterization; Thompson microphysics is used in the outer and inner domains.

Table 1: WRF simulations undertaken for this study, with grid spacing, start and end times.

Simulation	Start time	End Time	Grid spacing
D1A	2808 0000 UTC	3108 0000 UTC	12 km
D2A	2808 0600 UTC	3108 0000 UTC	4 km
D1B	2808 1200 UTC	3108 0000 UTC	12 km
D2B	2808 1800 UTC	3108 0000 UTC	4 km
D1C	2908 0000 UTC	3108 0000 UTC	12 km
D2C	2908 0600 UTC	3108 0000 UTC	4 km

Surface stresses (taux and tauy, empiric formulation) are computed from WRF simulated ten-meter wind components and used for estimating the zonal Ekman transport with a focus on 30 August 2015 at various locations along the Senegalese coast (Figure 2a). We used values of $\rho_a = 1.2$ kg m^{-3}, and a dimensionless empirical drag coefficient ($Cd = 1.3 \times 10^{-3}$ [7]) Ekman transport (Q, $m^3 \cdot s^{-1} \cdot m^{-1}$) was calculated using the formulation of wind stress, seawater density ($\rho = 1000$ kg m^{-3}) and the Coriolis parameter f by means of:

$$\tau_x = \rho_a \cdot C_d \cdot \sqrt{u^2 + v^2} \cdot u \quad (1); \quad \tau_y = \rho_a \cdot C_d \cdot \sqrt{u^2 + v^2} \cdot v \quad (2)$$

$$Q_x = \frac{\tau_y}{f \cdot \rho} \quad (3); \quad Q_y = \frac{-\tau_x}{f \cdot \rho} \quad (4)$$

In these two formulations above, the Q_x respectively Q_y corresponds to the zonal respectively meridional Ekman transport components.

Preprints (www.preprints.org) | NOT PEER-REVIEWED | Posted: 12 November 2019 doi:10.20944/preprints201911.0125.v1

3. Results.

a. Environmental conditions of the genesis of Fred

During the night of 27 to 28 August 2015 a mesoscale convective system, embedded in an AEW trough, from Mali moved into southeastern Senegal. It quickly strengthens after crossing Kedegou Highlands (in the southeast of Senegal) and arrives at the coast in the morning of the 28 August. Convection gradually weakening during the day of 28 and the wave remains almost stationary near the Senegal and Guinea coasts. From 29 August 0000 to 0006 UTC, convection is regenerated by developing vortex (figure 3 (a-f)). Satellite observations show that the surface cyclonic circulation began at the same period and the system is quickly classified tropical depression by the national hurricanes (NHC) about 0000 on 30th August. The sensor of "Melax the buoy" located at 400 km north (14°20'°N,17°14'°W) of the disturbance also observed the effects are with neighboring surface wind speed records of 12m/s (about 24 knots), with the intensification of the disturbance (figure not shown).

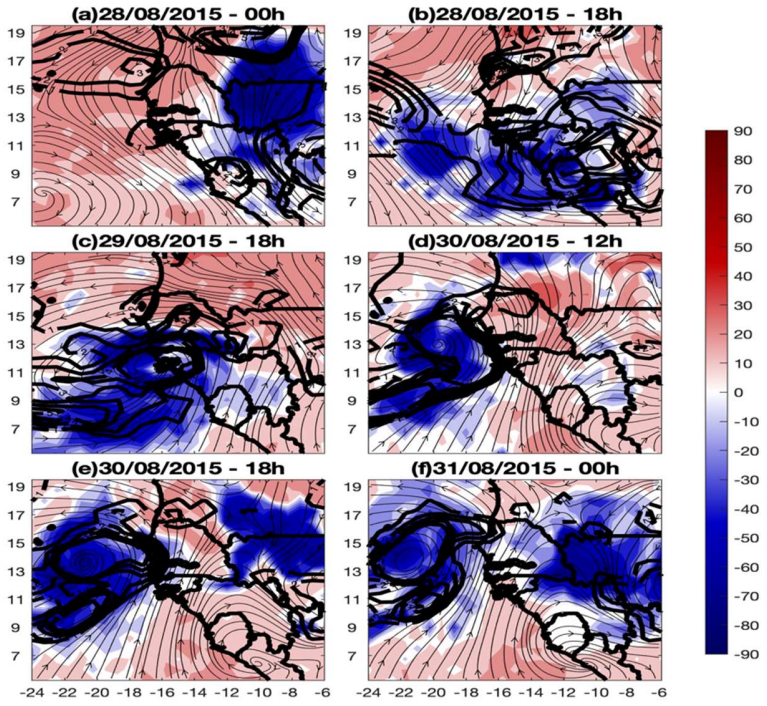

Figure 3 : MSG brightness temperature (in color), 850 hPa wind (in streamline) and relative vorticity (contours) showing the evolution of the disturbance that gave rise to the tropical storm Fred off the Senegal-Guinean coast

The disturbance developed in a favorable environment with ocean surface temperature higher than 28 C (figure 4). During 30 and 31 August, the system intensifies further to reach a category 1 hurricane on the Saphir-Simpson scale before reaching the Cape Verde Islands; a situation that never encountered during the 20th century with some evidence suggesting a hurricane in 1892 [1].

Preprints (www.preprints.org) | NOT PEER-REVIEWED | Posted: 12 November 2019 doi:10.20944/preprints201911.0125.v1

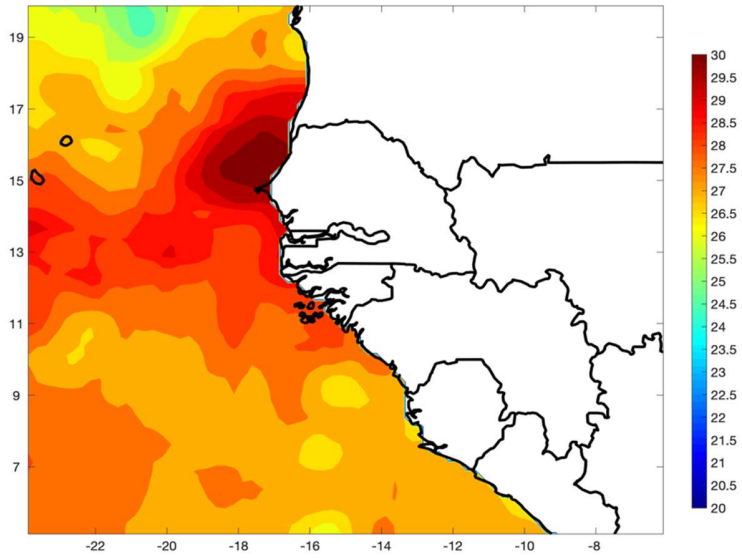

Figure 4: Mean daily Sea Surface Temperature of for August 30

Figures 5a-b shows DASCAT wind fields on 30 august and 31 august. Southerly winds occur near the Senegalese coast on 30 and 31 August. Winds of more than 25 knots are persistent during this period. The southerly fetch extends for more than 500 km for both days which would increase the wave heights beyond 4 meters on the coastlines to the south of Dakar especially during the morning hours of 31 August

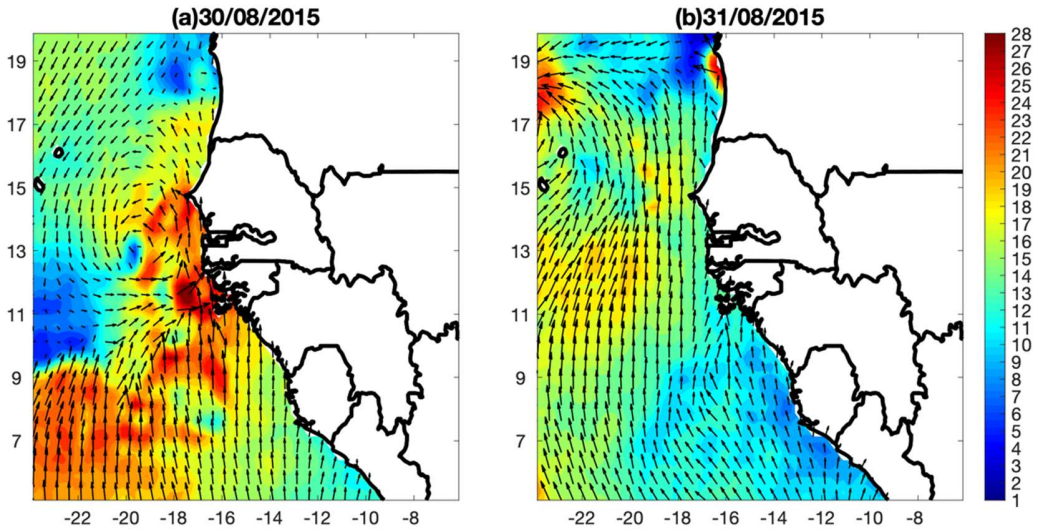

Figure 5: Mean daily 10m wind (colour and vector, in knots) in (a) for August 30 and in (b) for August 31.

b. Model evaluation

Tracks of the simulated disturbance relative to the NHC best track are presented on the figure 2a. In all of the simulations, the forecasted location of the storm is behind the official NHC location. Simulation D2A, which began on 28 August shows a track which is closest to the NHC track.

 doi:10.20944/preprints201911.0125.v1

However, its position at 0000 UTC 31 August is to the southeast of the actual location. It is approximately 6 hours behind the NHC position and located near the estimated NHC position at 1800 UTC, 30 August. Simulation D2B on the other hand, which begins at 1800 28 August, is displaced to the east of the NHC official track and located much closer to the Guinea-Bissau and Senegalese coastlines. Is it also displaced in time and occupies a latitude similar to D2A. The third simulation, D2C, begins at 0600, 29 August and is displaced to the west of the NHC position. It also occupies a biased position and is located at 14° N similar to the other two simulations at 0000 31 August. The differences in the simulated position of TC Fred, provide a useful means of evaluating coastal winds and the Ekman transport at the Palmerin, Rufisque, and Thiaroye Senegal which are at or near locations where damaged occurred (Figure 2b).

Figures 6 (a-f) represent simulated maximum reflectivity Radar and 10 m wind on August 30, 2015, respectively at 0600 UTC and 2000UTC. Simulated disturbances at 0600 UTC 30 August are located between 11 and 12.5N in the three simulations (Figures 3a, c, e). The simulated center of the disturbance in D2B is located closest to the coast (12.3N, 17W), while the center in D2C (11.7N, 18W) is located the furthest out to sea; the center of the disturbance in D2A is located further south near 11.3N. Winds of 30-40 knots are simulated in all simulations but cover a larger area in simulations D2A and D2B. At 2000 UTC, the centers of the simulated storms are located near 13.5N, 20.5W (D2A), 14.5N, 20W (D2B) and 13.5N, 21W (D2C) (Figures 6b, d, f). The strongest winds of 40-50 knots are found near the center of the simulated disturbances. The three simulations show strong southerly winds (20-30 knots) along the Senegalese coastlines at 2000 UTC. In the regions where damages were reported, southerly winds would drive waves northward towards the Senegalese coast.

Preprints (www.preprints.org) | NOT PEER-REVIEWED | Posted: 12 November 2019 doi:10.20944/preprints201911.0125.v1

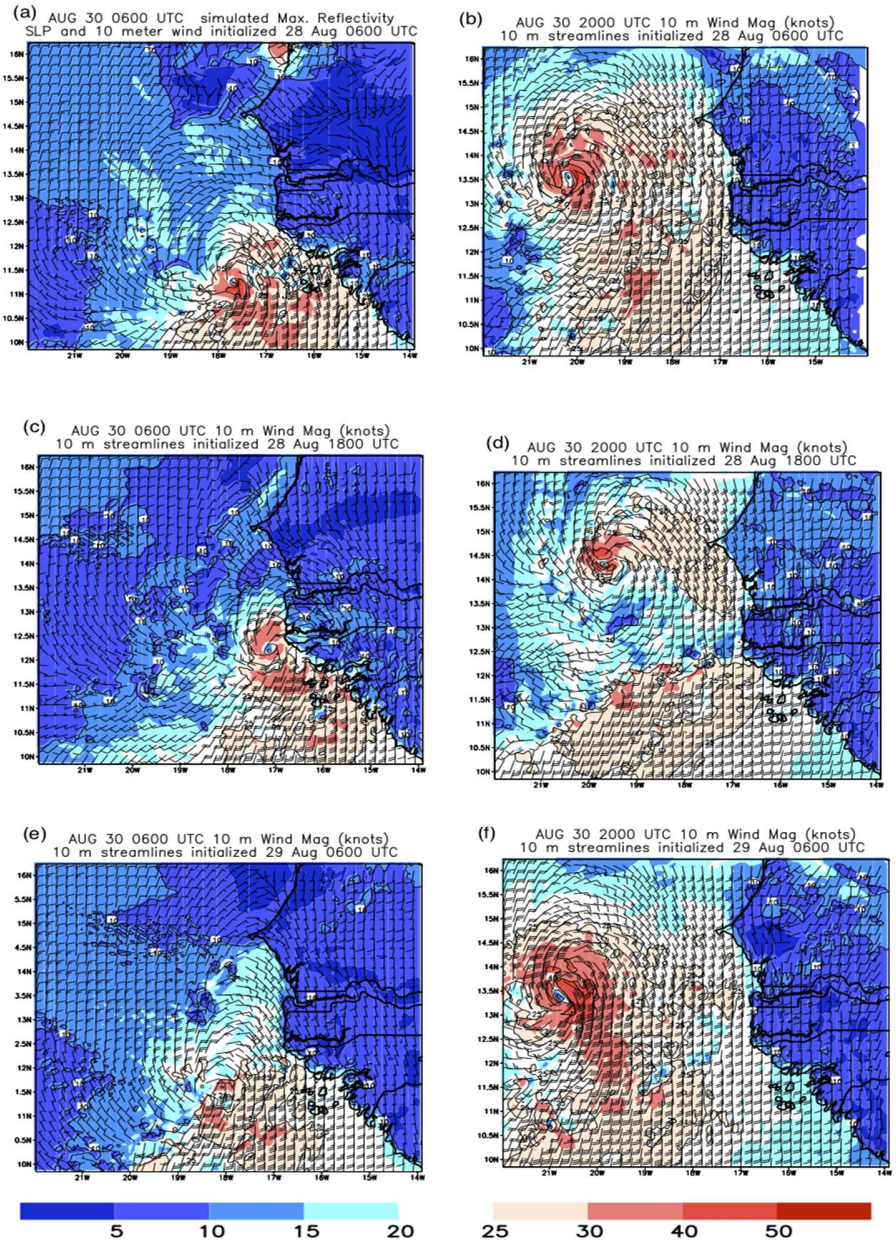

Figure 6: Simulated Maximum reflectivity Radar on August 30, 2015, respectively from left to right at 0600 UTC and 2000UTC. Top for simulation 2A, middle for simulation 2B and bottom for simulation 2C.

Figures 7a, b shows the observed and simulated meridional wind component at selected locations along coastal Senegal and WRF meridional winds at the nearest grid point of Dakar observation. It should be noted that, except for Dakar, all the other stations present discontinuities synonymous of a lack of data (figure 7a). At the southernmost station of Cap Skirring, a rapid transition to southerly winds are found on 30 August, beginning at 0600 UTC. Stations located further north also show a pattern of southerly winds after 0600 UTC at Banjul, Gambia, Dakar, and Ziguinchor Senegal. The wind speeds of 10-15 knots are found at Cap Skirring after 0600 UTC, while winds of 10 to 15 knots are found after 1200 UTC in Dakar, Senegal. This pattern of observed southerly winds between Cap Skirring and Dakar, Senegal (distance 142 nautical miles or 263 km)

Preprints (www.preprints.org) | NOT PEER-REVIEWED | Posted: 12 November 2019 doi:10.20944/preprints201911.0125.v1

would have created fetch that leading significant wave heights in coastal zones to the south of Dakar, Senegal based on the Sverdrup-Monk-Bretschneider Nomogram.

Simulated winds (figure 7b) in Dakar also show a pattern of southerly winds in agreement with observations. Simulation D2A shows continuous southerly winds beginning at approximately 0500 UTC, 30 August and continuing throughout the day. The winds reach the maximum value of 22 knots between 1600 and 2200 UTC. Simulation D2B shows a short period of southerly winds but produce the strongest simulated meridional winds of more than 25 knots between 2100 and 2300 UTC on 30 August. While the simulated disturbance is located furthest west relative to the other simulations, it simulated southerly winds beginning the earliest (0400 UTC on 30 August) and increases throughout the day, reaching its largest values between 1700 and 2200 UTC. Stronger simulated offshore southerly winds are expected because of the closer proximity to the tropical disturbance and consistent with observations of buoys and offshore winds being stronger than winds along the coast by a factor of 1.4 to 1.7 [19]

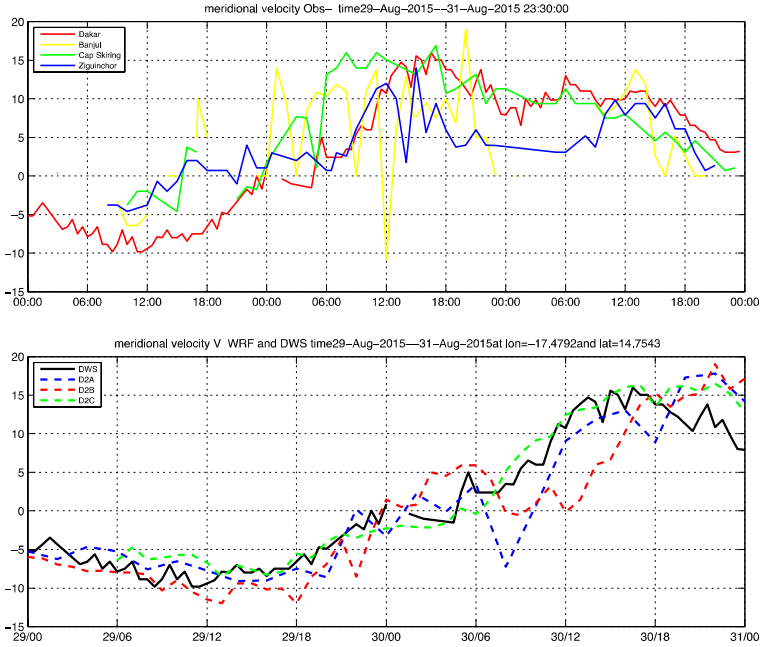

Figure 7: (a) observed of meridional wind component at selected locations along coastal Senegal: red (Dakar), yellow (Banjul) green Cap Skiring and blue Ziguinchor. (b) simulated WRF meridional winds at the nearest grid point of Dakar observation: blue dashed line for simulation 2A, red dashed line for 2B and green dashed line for 2C. The solid black line represents the observed meridional wind at Dakar

c. Zonal Ekman transport estimation

The zonal Ekman transport, which is determined from simulated meridional winds at grid-point locations near Palmerin, Rufisque, and Thiaroye is estimated using the equations (2 and 3). Zonal Ekman transport indicates increasing eastward transport towards the coastline after 1200 UTC, 30 August based on D2A and D2B (figure 8a-c). The largest transport occurs after 1800 UTC and is found at Rufisque relative to the other coastal locations in these simulations. Zonal transported estimated by simulation D3C is smaller relative to D2A and D2B. However, all of the

 doi:10.20944/preprints201911.0125.v1

transport is eastward in this simulation with the largest values found near 0000 30 August and steady westward transport between 0900 and 2000 UTC 30 August.

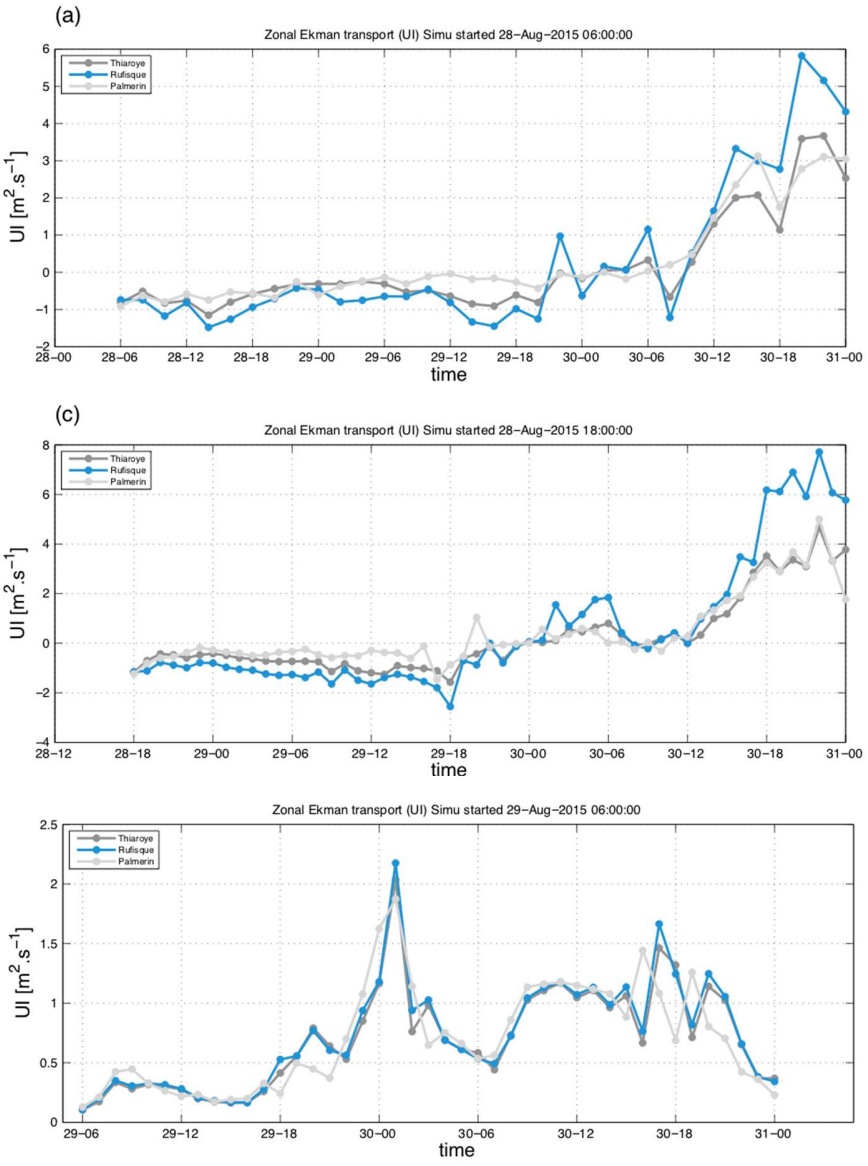

Figure 7: computed Zonal Ekman transport at grid-point locations near Palmerin, Rufisque, and Thiaroye

Figure 9 shows varied accumulated Ekman transport from the three simulations between Guinea and Dakar, Senegal. The accumulated Ekman transport computed from simulation D2A occurs to the south of Senegal (Figure 9a), while a higher accumulated Ekman transport is found in D2B and D2C along the Senegalese coastline (Figures 9b and 9c). The largest accumulated Ekman transport along the Senegalese coastline occurs in 2B which has to closer track to the coast.

Preprints (www.preprints.org) | NOT PEER-REVIEWED | Posted: 12 November 2019 doi:10.20944/preprints201911.0125.v1

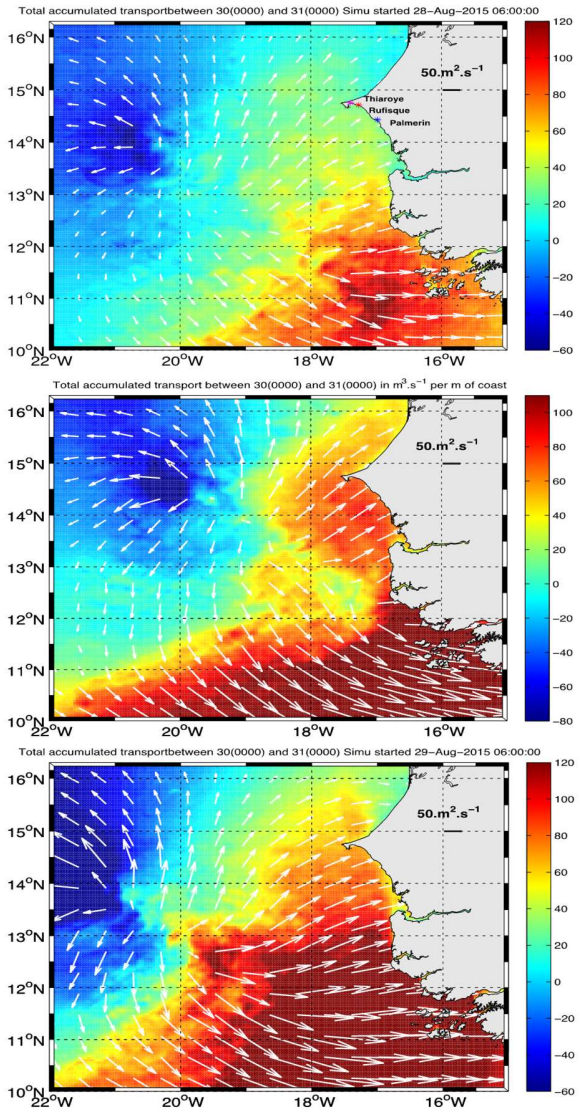

Figure 8: Zonal accumulated Ekman transport from 30th to 31st august for 2A (top), 2B (middle) and 2C (bottom. the arrows represent the Eckman transport direction

5. Conclusion

During the evening of 30 August and likely into the early morning hours, residents along the coast of Senegal from Dakar through Palmarin experienced coastal flooding and infrastructure associated the tropical disturbance which became Hurricane Fred. The flooding occurred with the tropical disturbance was developing but several hundred km away from the coast. Discussions with residents of Bargny spoke of rising seas throughout the night and early morning hours which caused the damage. Additional damage in the surrounding areas of Rufisque may have occurred (Ndoye, personal observation) but not reported. In this work, we used WRF to examine the potential impact of the tropical disturbance with a focus on 30 August 2015. The three simulations show a spread in the storm tracks relative to the NHC official track, with simulation D2A which was initiated on 28 August 0000 UTC having the smallest track errors. Simulation D2B had an eastward bias, while simulation D2C had a westward bias.

Observations between Dakar and southern Senegal and including the Gambia show southerly winds during the morning through the night of 30 August with model simulations showing agreement with the coastal observations. Satellite overpasses show winds greater than 15 knots along coastal Senegal for 30-31 August, which would create a long fetch. The southerly winds may have impacted the coast of Senegal through eastward Ekman. The use of a Munk-Sverdrup-Bretschneider nanogram suggests that a fetch of more 400 km for more than 24 hours with wind speeds of 20 knots would produce wave heights of more than 2 meters along coastal zones south of Dakar, Senegal.

The simulations associated with this tropical disturbance show that the damaging waves could occur even if the storm is not close to the Senegal coast. The shape of the Senegal coasts makes it vulnerable to strong southerly winds, which have a long fetch and duration. Similarly, [20] show that anti-cyclonic and cyclonic systems are responsible for extreme waves in the British Isles. In Senegal south of Dakar, developing low pressure associated with African Easterly Waves during the summer can produce southerly winds and thus serve as the source of extreme waves. High pressure can produce northerly winds and would serve as the source of extreme waves in coastal regions to the north of Dakar. These weather events can be predicted with some degree of success, although the prediction of tropical cyclo-genesis is still challenging across the extreme eastern Atlantic Ocean.

Increased Earth observations and predictive weather and wave models provide the best means of understanding events that cause coastal damage along West Africa. Such a system can provide the basis for developing a coastal warning system to protect the millions of people that live in coastal zones in West Africa in large cities, small towns, and fishing villages. The present challenge is to increase in situ coastal data, which has limited real-time buoy data and coastal weather station data. This data is needed to monitor extreme events, evaluate and improve satellite-based products, weather, and wave models.

Acknowledgments. This work was funded by Science for Weather Information and Forecasting Techniques (SWIFT) AND The African Monsoon Multidisciplinary Analysis (AMMA) 2050. The reanalyses data were obtained from the Institut Pierre Simon Laplace (IPSL; http://www. ipsl.fr/).

References

1. Foltz, G.R.; Schmid, C.; Lumpkin, R. An Enhanced PIRATA Dataset for Tropical Atlantic Ocean–Atmosphere Research. *J. Clim.* **2018**, *31*, 1499–1524.

2. Jenkins, G.S.; Brito, E.; Soares, E.; Chiao, S.; Lima, J.P.; Tavares, B.; Cardoso, A.; Evora, F.; Monteiro, M. Hurricane Fred (2015): Cape Verde's First Hurricane in Modern Times: Observations, Impacts, and Lessons Learned. *Bull. Am. Meteorol. Soc.* **2017**, *98*, 2603–2618.

3. Lafore, J.-P.; Beucher, F.; Peyrillé, P.; Diongue-Niang, A.; Chapelon, N.; Bouniol, D.; Caniaux, G.; Favot, F.; Ferry, F.; Guichard, F.; et al. A multi-scale analysis of the extreme rain event of Ouagadougou in 2009. *Q. J. R. Meteorol. Soc.* **2017**, *143*, 3094–3109.

4. Engel, T.; Fink, A.H.; Knippertz, P.; Pante, G.; Bliefernicht, J. Extreme Precipitation in the West African Cities of Dakar and Ouagadougou: Atmospheric Dynamics and Implications for Flood Risk Assessments. *J. Hydrometeorol.* **2017**, *18*, 2937–2957.

5. Sall, S.M.; Sauvageot, H. Cyclogenesis off the African Coast: The Case of Cindy in August 1999. *Mon. Weather Rev.* **2005**, *133*, 2803–2813.

6. DIAW, A.T. Morphométrie du littoral sintgalais et gambien. *Notes Afr.* 1984, 58–63.

7. Roy, C. Fluctuation of wind and upwelling variability off the Senegalese coast. *Ocean. Acta* **1989**, *12*, 361–369.

8. Ndoye, S.; Capet, X.; Estrade, P.; Sow, B.; Dagorne, D.; Lazar, A.; Gaye, A.; Brehmer, P. SST patterns and dynamics of the southern Senegal-Gambia upwelling center. *J Geophys Res* **2014**, *119*, 8315–8335.

9. Ndoye, S. Fonctionnement dynamique du centre d'upwelling sud-sénégalais: approche par la modélisation réaliste et l'analyse d'observations satellite de température de la mer. PhD Thesis, Université Pierre et Marie Curie, 2016.

10. Capet, X.; Estrade, P.; Machu, E.; Ndoye, S.; Grelet, J.; Lazar, A.; Marié, L.; Dausse, D.; Brehmer, P. On the dynamics of the southern Senegal upwelling center: observed variability from synoptic to super-inertial scales. *J. Phys. Oceanogr. 47*, 155–180.

11. Arnault, J.; Roux, F. Characteristics of African easterly waves associated with tropical cyclogenesis in the Cape Verde Islands region in July–August–September of 2004–2008. **2011**, *100*, 61–82.

12. Dieng, A.L.; Eymard, L.; Sall, S.M.; Lazar, A.; Leduc-Leballeur, M. Analysis of Strengthening and Dissipating Mesoscale Convective Systems Propagating off the West African Coast. *Mon. Weather Rev.* **2014**, *142*, 4600–4623.

13. Ndeye Astou Niang Dynamique socio-environnementale et développement local des régions côtières du Sénégal : l'exemple de la pêche artisanale. thesis, University of Rouen, 2009.

14. Bentamy, A.; Fillon, D.C. Gridded surface wind fields from Metop/ASCAT measurements. *Int. J. Remote Sens.* **2012**, *33*, 1729–1754.

15. Dee, D.P.; Uppala, S.M.; Simmons, A.J.; Berrisford, P.; Poli, P.; Kobayashi, S.; Andrae, U.; Balmaseda, M.A.; Balsamo, G.; Bauer, P.; et al. The ERA-Interim reanalysis: configuration and performance of the data assimilation system. *Q. J. R. Meteorol. Soc.* **2011**, *137*, 553–597.

16. Reynolds, R.W.; Smith, T.M.; Liu, C.; Chelton, D.B.; Casey, K.S.; Schlax, M.G. Daily High-Resolution-Blended Analyses for Sea Surface Temperature. *J. Clim.* **2007**, *20*, 5473–5496.

17. Ndoye, S.; Capet, X.; Estrade, P.; Sow, B.; Machu, E.; Brochier, T.; Döring, J.; Brehmer, P. Dynamics of a "low-enrichment high-retention" upwelling center over the southern Senegal shelf. *Geophys. Res. Lett.* **2017**, n/a–n/a.

18. Skamarock, C.; Klemp, B.; Dudhia, J.; Gill, O.; Barker, D.; Duda, G.; Huang, X.; Wang, W.; Powers, G. A Description of the Advanced Research WRF Version 3. **2008**.

19. Hsu, S.A., On the correction of land-based wind measurements for oceanographic applications 1980, 708–724.

20. Bell, R.J.; Gray, S.L.; Jones, O.P. North Atlantic storm driving of extreme wave heights in the North Sea. *J. Geophys. Res. Oceans* **2017**, *122*, 3253–3268.